

The explicit β_1/β_2 -Bathe time integration method

Mohammad Mahdi Malakiyeh^a, Saeed Shojaee^a, Saleh Hamzehei-Javaran^a,
Klaus-Jürgen Bathe^{b,*}

^a Department of Civil Engineering, Shahid Bahonar University of Kerman, Kerman, Iran

^b Massachusetts Institute of Technology Cambridge, MA 02139, United States



ARTICLE INFO

Article history:

Received 13 March 2023

Accepted 22 May 2023

Keywords:

Wave propagations

Direct time integration

Explicit integration

β_1/β_2 -Bathe method

Stability and solution accuracy

Numerical damping

ABSTRACT

In this paper we introduce the explicit β_1/β_2 -Bathe method for solving dynamic problems, in particular wave propagations. Like for the implicit β_1/β_2 -Bathe method, the proposed explicit scheme uses two sub-steps per time step and can be used directly as a first-order and a second-order method with the capability to suppress high spurious frequency response. In both sub-steps, standard Taylor series are employed resulting in an explicit solution scheme. The novelty is that we calculate the final displacements and velocities in each sub-step by applying correction terms using the generalized trapezoidal rule with control parameters β_1 and β_2 . This approach makes the method a quite simple scheme. We consider the stability, accuracy and numerical dispersion and give recommendations on the parameter values β_1 and β_2 to be used in practice. We give the solutions of four problems, three of which are wave propagation problems, and compare the results with those obtained using other methods. While more experience in the use of the procedure is needed to understand its full solution capabilities, we can already conclude that the proposed method is effective in some wave propagation analyses.

© 2023 Elsevier Ltd. All rights reserved.

1. Introduction

For the solution of dynamic problems in practice, numerical methods are generally the only option available to solve the equations of motion. Among the available numerical methods, the direct time integration methods are widely used. Direct time integration methods can be divided into two categories; in terms of stability, we have unconditionally stable and conditionally stable methods, and in terms of the formulation used, we have explicit and implicit schemes. If the method is not constrained by a stability condition for choosing the size of the time step, the method is termed unconditionally stable; otherwise, it is conditionally stable [1–3].

The most important differences between explicit and implicit methods are the stability of these methods and their computational costs [1–30]. An implicit time integration method can be conditionally or unconditionally stable, while explicit methods are always conditionally stable [1]. If diagonal mass and damping matrices are used, the explicit methods generally require less computational effort in each time step than the implicit methods. Since using an unconditionally stable implicit method, much larger time steps can in principle be used, it can be difficult to decide whether

an explicit or implicit method is more effective for the overall solution.

However, there are problem solutions in which an explicit method can clearly be more effective – namely, when the applied loads or the response to be calculated require a small time step. This is frequently the case in the solution of wave propagations, namely when a small time step of the order of the stability limit of an explicit solution scheme is inherently needed.

To achieve an accurate solution of wave propagations, the direct time integration should contain some numerical damping to prevent spurious response, see for example Refs. [1,8,12,17] and this numerical damping should ideally be optimal, that is, allow as large a time step as possible for an accurate solution.

Among the implicit methods, the β_1/β_2 -Bathe method can be very effective in solving wave propagation problems, but it is an implicit scheme. The excellent performance is due to using two sub-steps with two parameters β_1 and β_2 to impose numerical damping, and use the method as a first-order or a second-order scheme [17,18], see also Ref. [12].

Our objective in this paper is to present an efficient explicit time integration method – the explicit β_1/β_2 -Bathe method. This scheme also uses two sub-steps as does the implicit β_1/β_2 -Bathe method, and can also directly be employed as a first-order or a second-order method. Indeed, the control parameters β_1 and β_2 are used to obtain the first-order or second-order scheme and to numerically suppress the response due to high spurious

* Corresponding author.

E-mail address: kjb@mit.edu (K.-J. Bathe).

frequencies. The use of a first-order scheme can be of advantage in the solution of wave propagations [17,18].

The first explicit time integration method based on the use of sub-steps as employed in the implicit Bathe method [10–12] was proposed by G. Noh and K.J. Bathe [19]. The Noh-Bathe method uses numerical damping in the framework of the Bathe implicit scheme to suppress spurious response due to spurious high frequencies. We use the Noh-Bathe method in this paper to illustrate the response calculated with that scheme versus using the new scheme and show that the new explicit β_1/β_2 -Bathe method complements and is a further development of the earlier work. An important point is that the explicit β_1/β_2 -Bathe method can directly be used as a first-order scheme (like the implicit β_1/β_2 -Bathe method) and then also shows good performance.

In the following sections, we first present the governing equations used in the new scheme. Then we study the consistency, stability, order of accuracy, amplitude decay and period elongation. Finally, we illustrate the performance of the scheme through the solution of four example problems, also comparing the results obtained with those calculated using other schemes. We conclude that based on the solutions obtained the explicit β_1/β_2 -Bathe method can be effective for the solution of wave propagations.

2. The governing equations of the explicit β_1/β_2 -Bathe method

The proposed method uses two sub-steps, with the size of the first sub-step $\gamma\Delta t$ and the size of the second sub-step $(1-\gamma)\Delta t$. In each sub-step, we use standard Taylor series to solve for the unknown accelerations, after which we obtain the velocities and displacements by applying correction terms using the generalized trapezoidal rule (as employed in the Newmark method [1,4]) with the parameters β_1 for the velocities and β_2 for the displacements. We use different labels for the constants from those used in the Newmark method because the β_1 and β_2 are not constants for stability but simply constants used in correction terms to achieve good accuracy (but then naturally also affecting stability).

Considering linear analysis, in the first sub-step the equations of motion at time $t + \gamma\Delta t$ are

$$\mathbf{M}^{\text{t}+\gamma\Delta\text{t}}\ddot{\mathbf{U}} + \mathbf{C}^{\text{t}+\gamma\Delta\text{t}}\dot{\mathbf{U}} + \mathbf{K}^{\text{t}+\gamma\Delta\text{t}}\mathbf{U} = \text{}^{\text{t}+\gamma\Delta\text{t}}\mathbf{R} \quad (1)$$

where \mathbf{M} , \mathbf{C} and \mathbf{K} are the mass, damping and stiffness matrices; \mathbf{U} and \mathbf{R} represent the vector of nodal displacements/rotations and the load vector, respectively, and an over dot denotes a time derivative.

The truncated Taylor series expansions give

$$\text{}^{\text{t}+\gamma\Delta\text{t}}\dot{\mathbf{U}} = \text{}^{\text{t}}\dot{\mathbf{U}} + (\gamma\Delta\text{t})\text{}^{\text{t}}\ddot{\mathbf{U}} \quad (2)$$

and

$$\text{}^{\text{t}+\gamma\Delta\text{t}}\mathbf{U} = \text{}^{\text{t}}\mathbf{U} + (\gamma\Delta\text{t})\text{}^{\text{t}}\dot{\mathbf{U}} + (0.5)(\gamma\Delta\text{t})^2\text{}^{\text{t}}\ddot{\mathbf{U}} \quad (3)$$

Substituting Eqs. (2) and (3) into Eq. (1), we obtain

$$\mathbf{M}^{\text{t}+\gamma\Delta\text{t}}\ddot{\mathbf{U}} = \text{}^{\text{t}+\gamma\Delta\text{t}}\hat{\mathbf{R}}_1 \quad (4)$$

where

$$\begin{aligned} \text{}^{\text{t}+\gamma\Delta\text{t}}\hat{\mathbf{R}}_1 = & \text{}^{\text{t}+\gamma\Delta\text{t}}\mathbf{R} - \mathbf{C} \left[\text{}^{\text{t}}\dot{\mathbf{U}} + (\gamma\Delta\text{t})\text{}^{\text{t}}\ddot{\mathbf{U}} \right] \\ & - \mathbf{K} \left[\text{}^{\text{t}}\mathbf{U} + (\gamma\Delta\text{t})\text{}^{\text{t}}\dot{\mathbf{U}} + (0.5)(\gamma\Delta\text{t})^2\text{}^{\text{t}}\ddot{\mathbf{U}} \right] \end{aligned} \quad (5)$$

We note that in Eqs. (2) and (3), the accelerations $\text{}^{\text{t}+\gamma\Delta\text{t}}\ddot{\mathbf{U}}$ are not used.

The solution of Eq. (4) gives the accelerations at time $t + \gamma\Delta t$. Next, we use Eqs. (2) and (3) again but with the correction terms added that involve the just calculated accelerations and the parameters β_1 for the velocities and β_2 for the displacements

$$\text{}^{\text{t}+\gamma\Delta\text{t}}\dot{\mathbf{U}} = \text{}^{\text{t}}\dot{\mathbf{U}} + (\gamma\Delta\text{t})\text{}^{\text{t}}\ddot{\mathbf{U}} + \beta_1(\gamma\Delta\text{t}) \left(\text{}^{\text{t}+\gamma\Delta\text{t}}\ddot{\mathbf{U}} - \text{}^{\text{t}}\ddot{\mathbf{U}} \right) \quad (6)$$

$$\text{}^{\text{t}+\gamma\Delta\text{t}}\mathbf{U} = \text{}^{\text{t}}\mathbf{U} + (\gamma\Delta\text{t})\text{}^{\text{t}}\dot{\mathbf{U}} + (0.5)(\gamma\Delta\text{t})^2\text{}^{\text{t}}\ddot{\mathbf{U}} + \beta_2(\gamma\Delta\text{t})^2 \left(\text{}^{\text{t}+\gamma\Delta\text{t}}\ddot{\mathbf{U}} - \text{}^{\text{t}}\ddot{\mathbf{U}} \right) \quad (7)$$

The solution for the second sub-step is obtained in an analogous way. Hence the governing equations are for this sub-step

$$\mathbf{M}^{\text{t}+\Delta\text{t}}\ddot{\mathbf{U}} + \mathbf{C}^{\text{t}+\Delta\text{t}}\dot{\mathbf{U}} + \mathbf{K}^{\text{t}+\Delta\text{t}}\mathbf{U} = \text{}^{\text{t}+\Delta\text{t}}\mathbf{R} \quad (8)$$

$$\text{}^{\text{t}+\Delta\text{t}}\dot{\mathbf{U}} = \text{}^{\text{t}+\gamma\Delta\text{t}}\dot{\mathbf{U}} + (1-\gamma)(\Delta\text{t})\text{}^{\text{t}+\gamma\Delta\text{t}}\ddot{\mathbf{U}} \quad (9)$$

$$\text{}^{\text{t}+\Delta\text{t}}\mathbf{U} = \text{}^{\text{t}+\gamma\Delta\text{t}}\mathbf{U} + (1-\gamma)(\Delta\text{t})\text{}^{\text{t}+\gamma\Delta\text{t}}\dot{\mathbf{U}} + (0.5)(1-\gamma)^2(\Delta\text{t})^2\text{}^{\text{t}+\gamma\Delta\text{t}}\ddot{\mathbf{U}} \quad (10)$$

$$\mathbf{M}^{\text{t}+\Delta\text{t}}\ddot{\mathbf{U}} = \text{}^{\text{t}+\Delta\text{t}}\hat{\mathbf{R}}_2 \quad (11)$$

where

$$\begin{aligned} \text{}^{\text{t}+\Delta\text{t}}\hat{\mathbf{R}}_2 = & \text{}^{\text{t}+\Delta\text{t}}\mathbf{R} - \mathbf{C} \left[\text{}^{\text{t}+\gamma\Delta\text{t}}\dot{\mathbf{U}} + (1-\gamma)(\Delta\text{t})\text{}^{\text{t}+\gamma\Delta\text{t}}\ddot{\mathbf{U}} \right] \\ & - \mathbf{K} \left[\text{}^{\text{t}+\gamma\Delta\text{t}}\mathbf{U} + (1-\gamma)(\Delta\text{t})\text{}^{\text{t}+\gamma\Delta\text{t}}\dot{\mathbf{U}} + (0.5)(1-\gamma)^2(\Delta\text{t})^2\text{}^{\text{t}+\gamma\Delta\text{t}}\ddot{\mathbf{U}} \right] \end{aligned} \quad (12)$$

and then we obtain the final velocities and displacements at time $t + \Delta t$

$$\begin{aligned} \text{}^{\text{t}+\Delta\text{t}}\dot{\mathbf{U}} = & \text{}^{\text{t}+\gamma\Delta\text{t}}\dot{\mathbf{U}} + (1-\gamma)(\Delta\text{t})\text{}^{\text{t}+\gamma\Delta\text{t}}\ddot{\mathbf{U}} \\ & + \beta_1(1-\gamma)(\Delta\text{t}) \left(\text{}^{\text{t}+\Delta\text{t}}\ddot{\mathbf{U}} - \text{}^{\text{t}+\gamma\Delta\text{t}}\ddot{\mathbf{U}} \right) \end{aligned} \quad (13)$$

$$\begin{aligned} \text{}^{\text{t}+\Delta\text{t}}\mathbf{U} = & \text{}^{\text{t}+\gamma\Delta\text{t}}\mathbf{U} + (1-\gamma)(\Delta\text{t})\text{}^{\text{t}+\gamma\Delta\text{t}}\dot{\mathbf{U}} + (0.5)(1-\gamma)^2(\Delta\text{t})^2\text{}^{\text{t}+\gamma\Delta\text{t}}\ddot{\mathbf{U}} \\ & + \beta_2(1-\gamma)^2(\Delta\text{t})^2 \left(\text{}^{\text{t}+\Delta\text{t}}\ddot{\mathbf{U}} - \text{}^{\text{t}+\gamma\Delta\text{t}}\ddot{\mathbf{U}} \right) \end{aligned} \quad (14)$$

The above equations are used recursively to solve the equations of motion of the finite element system. Since the accelerations are not used in Eqs. (2) and (3), and (9) and (10), the scheme is an explicit integration method. We note that the scheme is quite simple, even when a banded damping matrix is used, which makes it an attractive solution method. However for good solution efficiency we usually need to use a lumped mass matrix (as in all explicit solution schemes).

We should note that in each sub-step the same procedures are used, but of course, for the sub-steps of sizes $\gamma\Delta t$ and $(1-\gamma)\Delta t$. Hence if we use $\gamma = 0.5$, as we shall do below, the two sub-steps use the same solution algorithms and we may look at this special case of the scheme as a one-step method.

Comparing the method with the explicit Noh-Bathe scheme, we see that the Eqs. (1) to (5) and Eqs. (8) to (12) are also used in the Noh-Bathe scheme but that the correction terms used in Eqs. (6), (7) and in Eqs. (13), (14) are in general different. These corrections are applied to calculate the new displacements and velocities at the end of the sub-step and the full step and involve the important parameters β_1 and β_2 .

3. Consistency and order of accuracy

To analyze the explicit β_1/β_2 -Bathe scheme, we formulate the method for a typical single degree of freedom equation [1]

$$\begin{bmatrix} \text{}^{\text{t}+\Delta\text{t}}\ddot{u} \\ \text{}^{\text{t}+\Delta\text{t}}\dot{u} \\ \text{}^{\text{t}+\Delta\text{t}}u \end{bmatrix} = \mathbf{A} \begin{bmatrix} \text{}^{\text{t}}\ddot{u} \\ \text{}^{\text{t}}\dot{u} \\ \text{}^{\text{t}}u \end{bmatrix} + \mathbf{L}_a^{\text{t}+\gamma\Delta\text{t}}r + \mathbf{L}^{\text{t}+\Delta\text{t}}r \quad (15)$$

where \mathbf{A} is the integration approximation operator, and \mathbf{L}_a and \mathbf{L} denote load operators. These operators are given in Appendix A, where in that appendix ω and ξ are the frequency of the undamped system and the damping ratio.

The order of accuracy quantifies the rate of convergence of the numerical solution to the exact solution and is given by the local truncation error

$$\tau = \frac{1}{\Delta t} [{}^{t+\Delta t}u - A_1 {}^t u + A_2 {}^{t-\Delta t}u - A_3 {}^{t-2\Delta t}u] \tag{16}$$

where A_1, A_2 and A_3 are the invariants of \mathbf{A}

$$\begin{aligned} A_1 &= \text{trace}(\mathbf{A}) \\ A_2 &= \frac{1}{2} \left((\text{trace}(\mathbf{A}))^2 - \text{trace}(\mathbf{A}^2) \right) \\ A_3 &= \det(\mathbf{A}) \end{aligned} \tag{17}$$

Expanding the terms in Eq. (16) about t and eliminating the second and higher order derivatives, the local truncation error is in general given by

$$\tau = e_1 \Delta t + e_2 \Delta t^2 + e_3 \Delta t^3 + O(\Delta t^4) \tag{18}$$

with the constants $e_i, i = 1, 2, 3, \dots$

For the explicit β_1/β_2 -Bathe method, the local truncation error is given by

$$\begin{aligned} \tau &= \left((2\beta_1 - 1)(\gamma^2 - \gamma + \frac{1}{2}) \left((1 - 4\xi^2) {}^t \dot{u} - 2\xi\omega {}^t u \right) \omega^2 \right) \Delta t^2 \\ &+ O(\Delta t^3) \end{aligned} \tag{19}$$

Therefore, since $e_1 = 0.0$, the method is consistent for any values of the parameters β_1 and β_2 . Considering the accuracy, using $\beta_1 \neq 0.5$, the method has first-order accuracy and using $\beta_1 = 0.5$, the method shows second-order accuracy.

4. Stability, period elongation and amplitude decay

The stability and accuracy of a time integration method can be investigated by calculating the spectral radius of the integration approximation operator, $\rho(\mathbf{A})$, and calculating the period elongation and amplitude decay [1].

For the explicit β_1/β_2 -Bathe method, the spectral radius is a function of $\beta_1, \beta_2, \xi, \gamma$ and $\Delta t/T$. The method is stable if $\rho(\mathbf{A}) \leq 1$ [1]. We consider the case $\xi = 0$ and $\gamma = 0.5$.

An important feature for an effective use of the method is to be able to choose the order of solution accuracy – choose the first or second order – and the time step size for applying numerical damping, that is, the time step size when the spectral radius rapidly decreases from the value of 1.

The stability analysis, performed like given for example in Refs. [1,7], shows that the explicit β_1/β_2 -Bathe method is conditionally stable, like all explicit methods, hence only stable if $\Delta t \leq \Delta t_{cr}$, where Δt_{cr} is the critical time step. The maximum critical time step

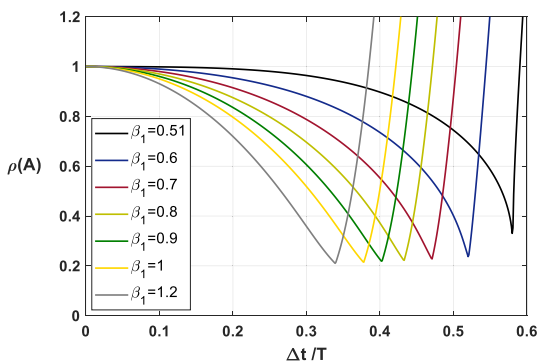


Fig. 1. Spectral radius of the explicit β_1/β_2 -Bathe method with $\beta_2 = 0.07\beta_1$ (first region).

value of the proposed method is twice that of the central difference method, like for the Noh-Bathe method.

Further analysis also shows that for two regions $\beta_1 = [0.51, 1.2]$ with $\beta_2 = 0.07\beta_1$, and $\beta_1 = 0.5$ with $\beta_2 = [0, 0.07]$, the method gives good accuracy. In the first region we have first-order accuracy and in the second region we have second-order accuracy.

Then in the first region, as we change the β_1 value from 0.51 to 1.2, the numerical damping is applied earlier; that is, Fig. 1 shows that with $\beta_1 = 0.51$ the spectral radius is longest close to 1. We also see that as β_1 increases, the amplitude decay and period elongation errors increase (see Figs. 2, 3).

Considering the second region, as we increase β_2 from 0 to 0.07 the numerical damping is applied earlier, the amplitude decay

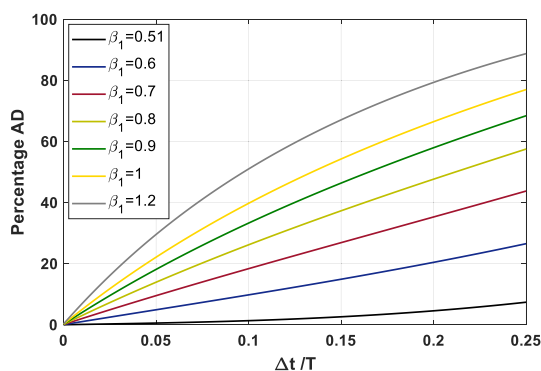


Fig. 2. Amplitude decay of the explicit β_1/β_2 -Bathe method with $\beta_2 = 0.07\beta_1$ (first region).

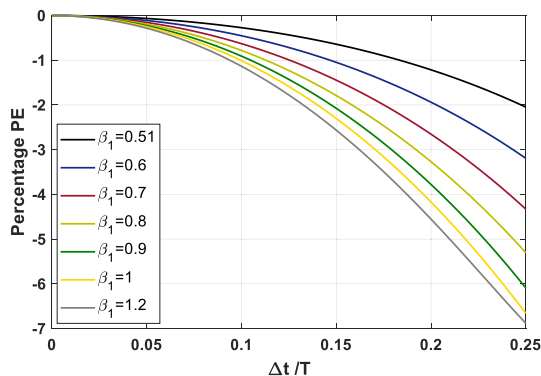


Fig. 3. Period elongation of the explicit β_1/β_2 -Bathe method with $\beta_2 = 0.07\beta_1$ (first region).

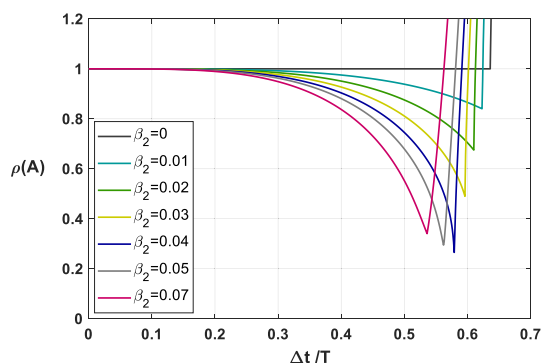


Fig. 4. Spectral radius of the explicit β_1/β_2 -Bathe method with $\beta_1 = 0.5$ (second region).

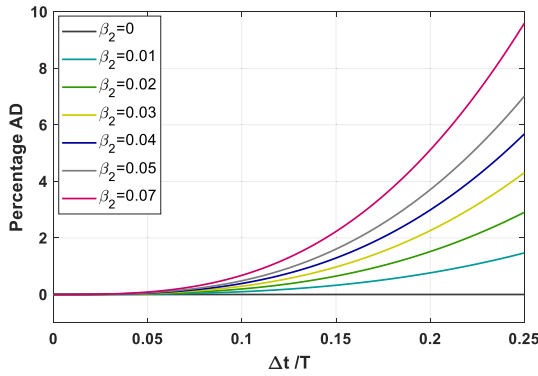


Fig. 5. Amplitude decay of the explicit β_1/β_2 -Bathe method for $\beta_1 = 0.5$ (second region).

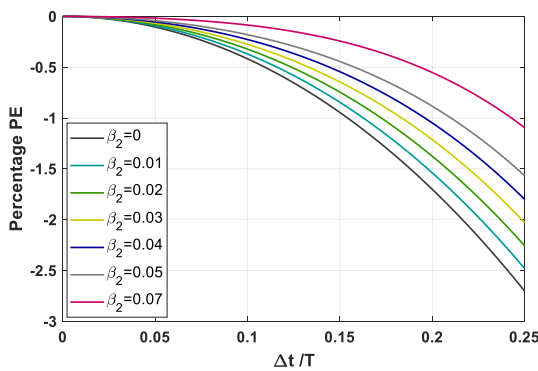


Fig. 6. Period elongation of the explicit β_1/β_2 -Bathe method for $\beta_1 = 0.5$ (second region).

error increases and the period elongation error decreases (see Figs. 4 to 6). Note that when $\beta_2 = 0$, no numerical damping is used.

We can compare these results with those given for the Noh-Bathe scheme in ref. [19], but of course only for the case of second-order accuracy (the Noh-Bathe scheme is second-order accurate). This comparison shows that the new second-order explicit β_1/β_2 -Bathe method gives about the same amplitude decays and period elongations as the Noh-Bathe method, see Figs. 5 and 6 and ref. [19].

5. Illustrative example solutions

In this section, we consider the solutions of four problems to illustrate the properties of the explicit β_1/β_2 -Bathe method. We

Table 1a

Values of parameters β_1 and β_2 for very good results, but the user needs to choose.

	explicit β_1/β_2 -Bathe method	implicit β_1/β_2 -Bathe method
wave propagations	$\beta_1 \in [0.51, 1.2], \beta_2 = 0.07\beta_1$	$\beta_1 \in (1/3, \infty), \beta_2 = 2\beta_1$
structural dynamics	$\beta_1 = 0.5, \beta_2 \in [0, 0.07]$	$\beta_1 \in [1/3, 0.5], \beta_2 = 1 - \beta_1$

Table 1b

Specific values of parameters β_1 and β_2 for (frequently) good results.

	explicit β_1/β_2 -Bathe method	implicit β_1/β_2 -Bathe method
wave propagations	$\beta_1 = 0.6, \beta_2 = 0.07\beta_1$	$\beta_1 = 0.39, \beta_2 = 2\beta_1$
structural dynamics	$\beta_1 = 0.5, \beta_2 = 0.04$	$\beta_1 = 1/3, \beta_2 = 1 - \beta_1$

compare the solutions obtained using the explicit β_1/β_2 -Bathe method with those obtained using the central difference, Noh-Bathe and implicit β_1/β_2 -Bathe methods. For all solutions obtained, we used the lumped mass matrix, except in Section 5.4 we employed the consistent mass matrix for the solution with the implicit β_1/β_2 -Bathe method. For the central difference method solutions, the starting procedure given in Ref. [1] was used.

For the solutions using the β_1/β_2 -Bathe methods, the values of the parameters β_1 and β_2 need to be chosen, and for optimal solutions these values seem to change slightly depending on the problem solved. We give in Table 1a suggestions for choosing the values for the parameters β_1 and β_2 . With values in those regions, very good response predictions may be obtained. However, in practice, a user needs specific values for “just” good results, which we therefore give in Table 1b. The values given in the tables assume that lumped and consistent mass matrices are used, respectively, for the explicit and implicit schemes, and the values are based on our experiences obtained so far.

Regarding the solution times taken using the new explicit scheme, we have not run yet very large problems, and have not used an optimized code, but the required computational time is estimated to be approximately the same as when using the Noh-Bathe scheme, both being explicit methods using two sub-steps for a full time step. Hence the solution time is also about the same as when using the central difference method with a time step half the size of the full step.

In each case of the problems solved below, the number of finite element equations is small and all solutions have been obtained with a small computational effort.

Clearly, for the solutions of the four problems considered below, by choosing different values of parameters and CFL many solutions can be generated. However, we need to focus here on the essence of the techniques and hence we use the central difference method with CFL = 1.0 or close thereto, the Noh-Bathe method with the recommended value of $p = 0.54$ [19], and choose for the explicit β_1/β_2 -Bathe method the same CFL as for the Noh-Bathe method. In addition, we also show briefly the effects of using other parameter values to illustrate how the explicit and implicit β_1/β_2 -Bathe methods perform.

In the following problem solutions we endeavored to obtain very good results using Table 1a which can lead to the values given in Table 1b.

5.1. A simple system with 2 degrees of freedom

The equilibrium equations of the system are

$$\begin{bmatrix} 2 & 0 \\ 0 & 1 \end{bmatrix} \begin{Bmatrix} \ddot{u}_1(t) \\ \ddot{u}_2(t) \end{Bmatrix} + \begin{bmatrix} 6 & -2 \\ -2 & 4 \end{bmatrix} \begin{Bmatrix} u_1(t) \\ u_2(t) \end{Bmatrix} = \begin{Bmatrix} 0 \\ 10 \end{Bmatrix} \quad (20)$$

Table 2
The displacement of the first degree of freedom.

Time	0.28	0.56	0.84	1.12	1.4	1.68	1.96	2.24	2.52	2.8	3.08	3.36
Analytical solution	0.003	0.038	0.176	0.486	0.996	1.657	2.338	2.861	3.052	2.806	2.131	1.157
explicit β_1/β_2 -Bathe ($\beta_1 = 0.5, \beta_2 = 0$)	0.002	0.036	0.174	0.486	1.001	1.668	2.353	2.874	3.057	2.798	2.108	1.125
implicit β_1/β_2 -Bathe ($\beta_1 = 0.5, \beta_2 = 1-\beta_1$)	0.004	0.041	0.179	0.486	0.987	1.637	2.31	2.835	3.041	2.82	2.173	1.221
Central difference	0	0.031	0.168	0.487	1.02	1.7	2.40	2.91	3.07	2.77	2.04	1.02
Trap. rule	0.007	0.051	0.189	0.485	0.961	1.58	2.23	2.76	3	2.85	2.28	1.4

Table 3
The displacement of the second degree of freedom.

Time	0.28	0.56	0.84	1.12	1.4	1.68	1.96	2.24	2.52	2.8	3.08	3.36
Analytical solution	0.382	1.412	2.781	4.094	4.996	5.291	4.986	4.277	3.458	2.806	2.484	2.489
explicit β_1/β_2 -Bathe ($\beta_1 = 0.5, \beta_2 = 0$)	0.384	1.42	2.793	4.106	5	5.283	4.966	4.25	3.435	2.798	2.495	2.515
implicit β_1/β_2 -Bathe ($\beta_1 = 0.5, \beta_2 = 1-\beta_1$)	0.377	1.396	2.756	4.069	4.986	5.304	5.025	4.329	3.503	2.825	2.466	2.439
Central difference	0.392	1.45	2.83	4.14	5.02	5.26	4.9	4.17	3.37	2.78	2.54	2.60
Trap. rule	0.364	1.35	2.68	4	4.95	5.34	5.13	4.48	3.64	2.90	2.44	2.31

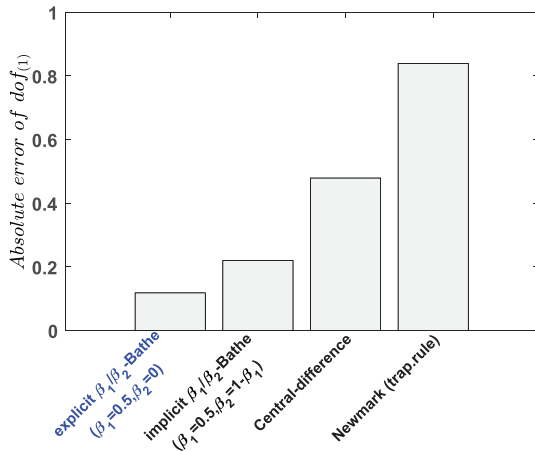


Fig. 7. Absolute error in u_1 .

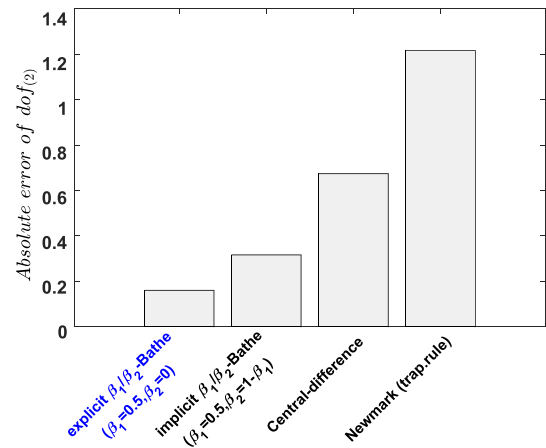


Fig. 8. Absolute error in u_2 .

and we assume that the initial displacements and velocities are zero. This is a very simple example problem to solve and we consider it only to indicate that when using an “acceptable” time step size for an explicit method may lead to a more accurate solution than using the same time step size with an implicit scheme.

With the central difference, trapezoidal rule, implicit β_1/β_2 -Bathe and explicit β_1/β_2 -Bathe methods we use $\Delta t = 0.28$, a time step size leading to stable results with the central difference method and the new explicit scheme, for which we could actually use almost twice the time step size. Also, the control parameters for each numerical method are selected in such a way that no numerical damping is applied.

We compare the numerical solutions with the analytical result for the displacement response. The analytical solution is

$$\begin{aligned} \hat{u}_1(t) &= \frac{2 \cos(\sqrt{5}t)}{3} - \frac{5 \cos(\sqrt{2}t)}{3} + 1 \\ \hat{u}_2(t) &= 3 - \frac{4 \cos(\sqrt{5}t)}{3} - \frac{5 \cos(\sqrt{2}t)}{3} \end{aligned} \quad (21)$$

The absolute error is given by

$$\text{Absolute error of dof}_{(j)} = \sum_{i=1}^n |\hat{u}_j(t_i) - \tilde{u}_j(t_i)| \quad (22)$$

where j denotes the degree of freedom considered, n denotes the number of steps, \hat{u}_j is the analytical solution and \tilde{u}_j is the numerical solution.

The displacement solutions obtained with the explicit β_1/β_2 -Bathe method and the other methods are listed in Tables 2 and 3. We recall that the solutions using the Noh-Bathe method with $p = 0.5$ are equal to those of the proposed method since the case of $\gamma = 0.5$ and $\beta_1 = 0.5, \beta_2 = 0$ is considered (that is, for this specific case, the equations used correspond to those used in the Noh-Bathe scheme).

Figs. 7 and 8 show the absolute errors. As seen, the errors using the central difference method are much less than those using the Trapezoidal Rule and the errors using the explicit β_1/β_2 -Bathe are less than using the implicit β_1/β_2 -Bathe method (both schemes employ two sub-steps). These results indicate – as we might expect – that when using the same time step size, the use of explicit methods may lead to more accurate solutions than using implicit schemes.

5.2. A clamped bar subjected to a step end load

We consider the clamped bar shown in Fig. 9 with the material and geometrical properties $E = 30 \times 10^6$ psi, $\rho = 0.00073$ lb/in³,

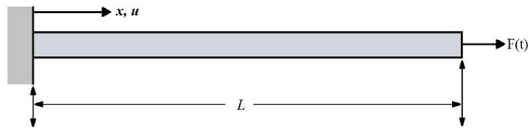


Fig. 9. A clamped-free bar subjected to a step end load [17].

$A = 1 \text{ in}^2$, and $L = 200 \text{ in}$. The bar is initially at rest, when the step end load $F(t) = 10,000 \text{ lb}$ is suddenly applied. We use 1000 equal 2-node elements with

$$\Delta t = (9.88 \times 10^{-7}) \times \text{CFL}$$

Figs. 10 to 12 give the predicted velocity response at the mid-point of the bar (node 500). We consider a longer time response and see significant spurious oscillations at the later time (Fig. 10). We use in Fig. 10 a slightly smaller CFL than 1.0 because of the rounding used to obtain the above relation for Δt . The predicted response using the Noh-Bathe method (Fig. 11) with the recommended $p = 0.54$ is better but also shows oscillations [19].

With the explicit β_1/β_2 -Bathe method using $\beta_1 = 0.51$ and $\beta_2 = 0.07\beta_1$, and the same CFL as used with the Noh-Bathe method (Fig. 12) we obtain an accurate solution with only some very small spurious oscillations.

In Fig. 13 we show that the explicit β_1/β_2 -Bathe method performs also well when using a smaller CFL, namely CFL = 1.0. Here we increased β_1 to 0.52. We include this solution to show that the method gives still reasonable results even with a smaller CFL than used in Fig. 12. As is well known, explicit schemes may perform considerably worse when the time step is reduced.

Finally, we compare in Figs. 14 and 15 the solutions obtained with the explicit and implicit β_1/β_2 -Bathe methods. The schemes show a similar high accuracy for the initial response, with the explicit β_1/β_2 -Bathe method giving a slightly better result, but this increase in accuracy is almost negligible.

The solutions in these figures have been obtained using the first-order explicit β_1/β_2 -Bathe method and show that for this problem solution the method performs well even when the response over longer time spans is sought.

5.3. A bi-material rod subjected to a step end load

We consider a rod of two pieces with different material properties, see Fig. 16. The Young's moduli are $E_1 = 8 \times 10^3 \text{ Pa}$ and $E_2 = 8 \times 10^2 \text{ Pa}$. The same Poisson's ratio ($\nu_1 = \nu_2 = 0$) and density ($\rho_1 = \rho_2 = 1 \text{ kg/m}^3$) are assumed for each region. The wave speeds in the regions are $c_1 = \sqrt{E_1/\rho_1}$ and $c_2 = \sqrt{E_2/\rho_2}$.

The rod is at rest when suddenly a uniform constant step traction of unit magnitude is applied at its right end.

In this study, the number of equal size 4- node two-dimensional elements for discretizing the spatial domain is 1×800 (with 400 elements in each piece) with the time-step

$$\Delta t = \text{CFL} \times \frac{\Delta x}{c_1} = \text{CFL} \times \frac{0.005}{40\sqrt{5}}$$

The stress and velocity predictions at point A are of interest.

Figs. 17 to 28 show the solutions obtained. As expected, the response predictions using the central difference method show significant spurious oscillations. The Noh-Bathe scheme employed with $p = 0.54$ also shows significant oscillations. Using the explicit

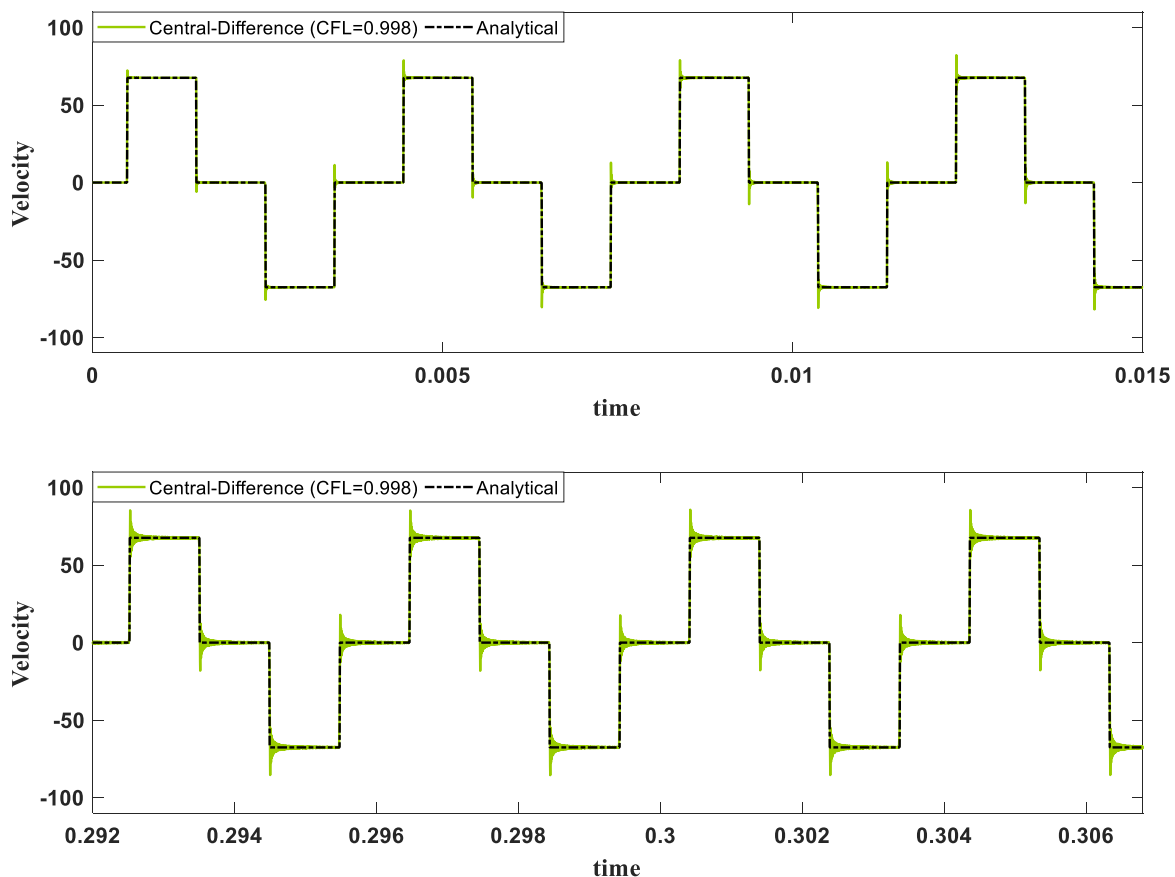


Fig. 10. Predicted velocity at mid-point of rod using Central-Difference method.

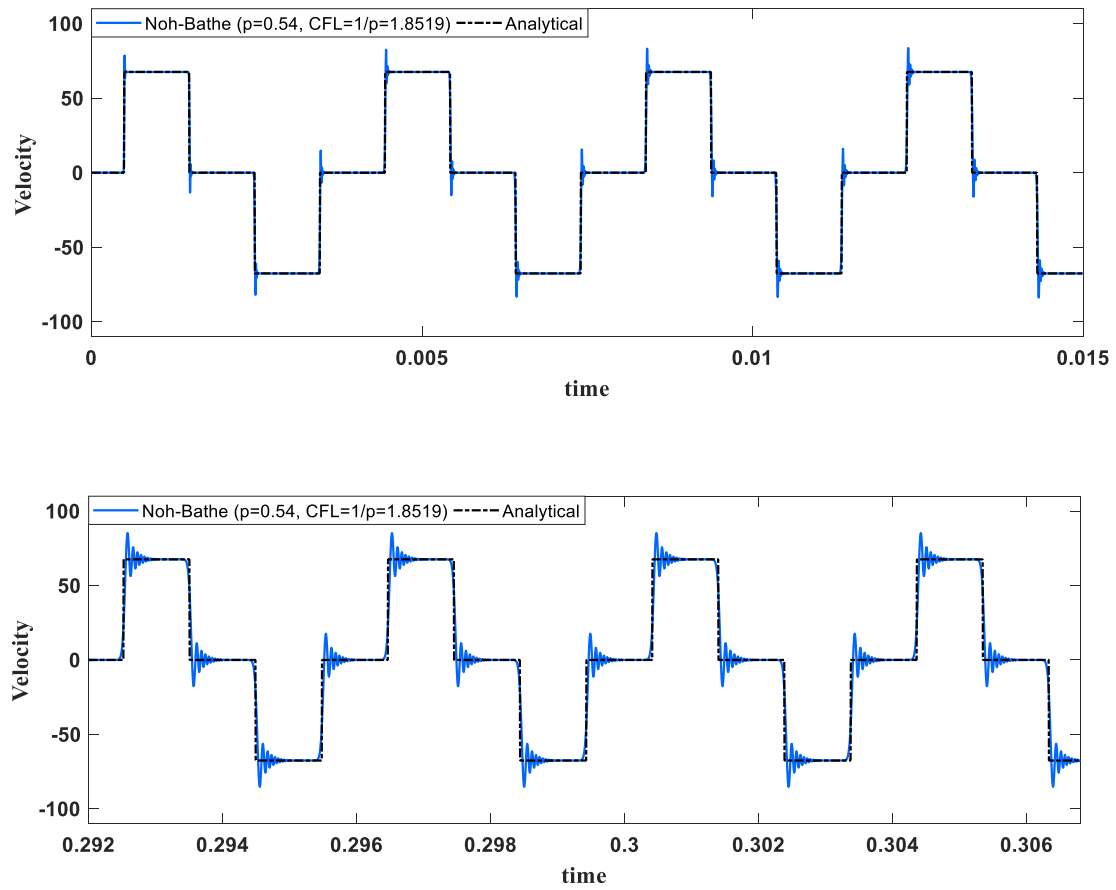


Fig. 11. Predicted velocity at mid-point of rod using Noh-Bathe method, CFL = 1.8519.

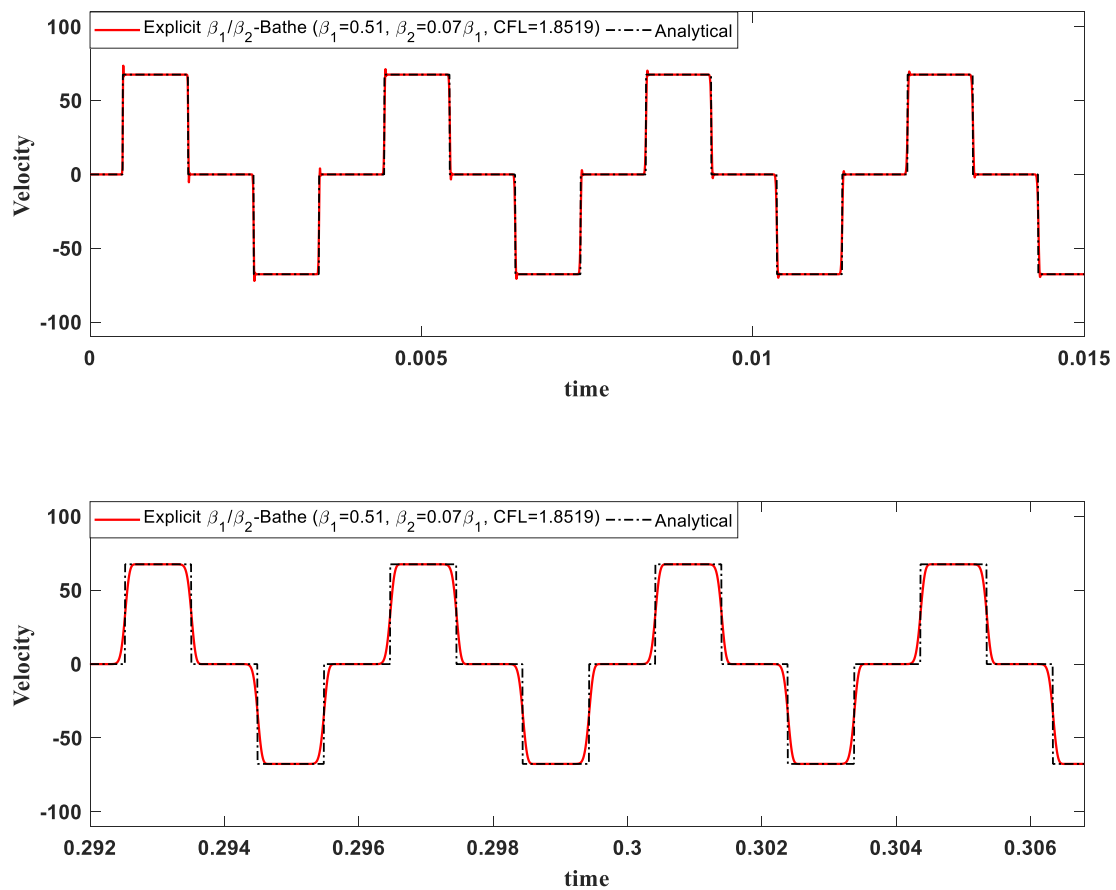


Fig. 12. Predicted velocity at mid-point of rod using explicit β_1/β_2 -Bathe method, $\beta_1 = 0.51$, CFL = 1.8519.

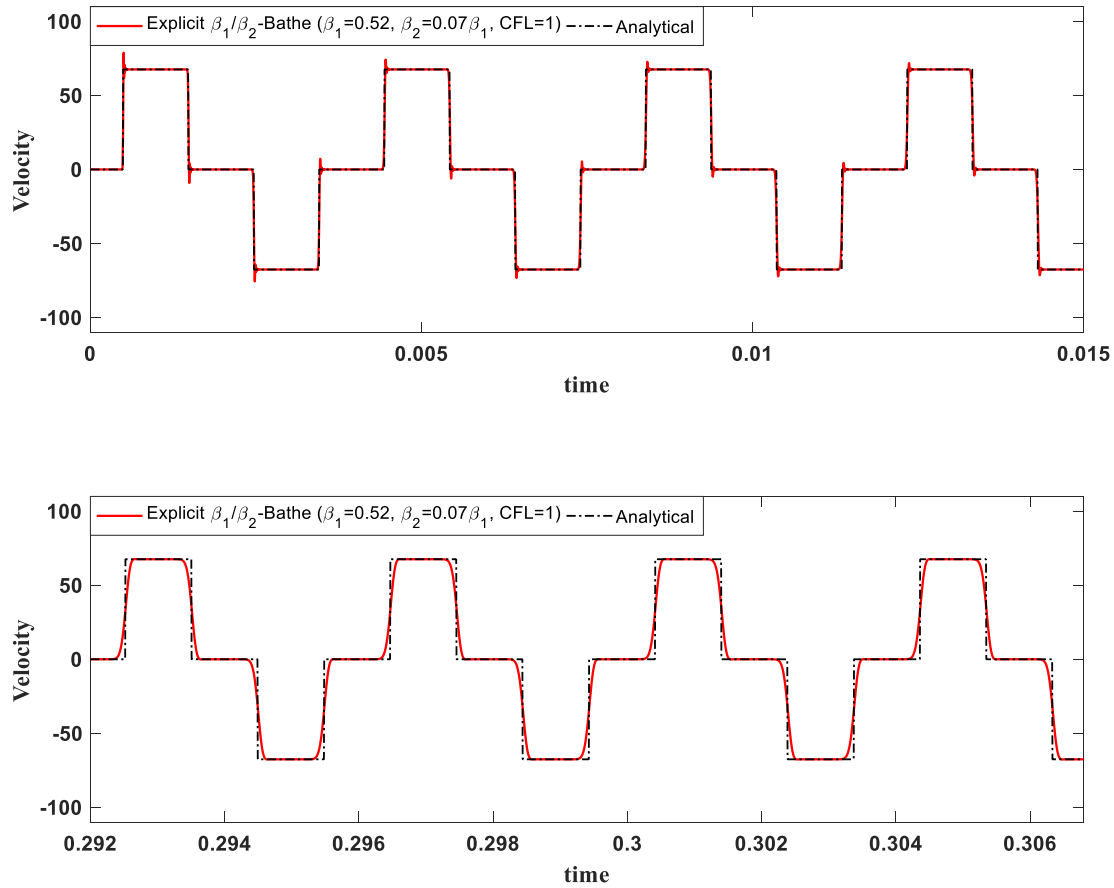


Fig. 13. Predicted velocity at mid-point of rod using explicit β_1/β_2 -Bathe method, $\beta_1 = 0.52$, CFL = 1.0.

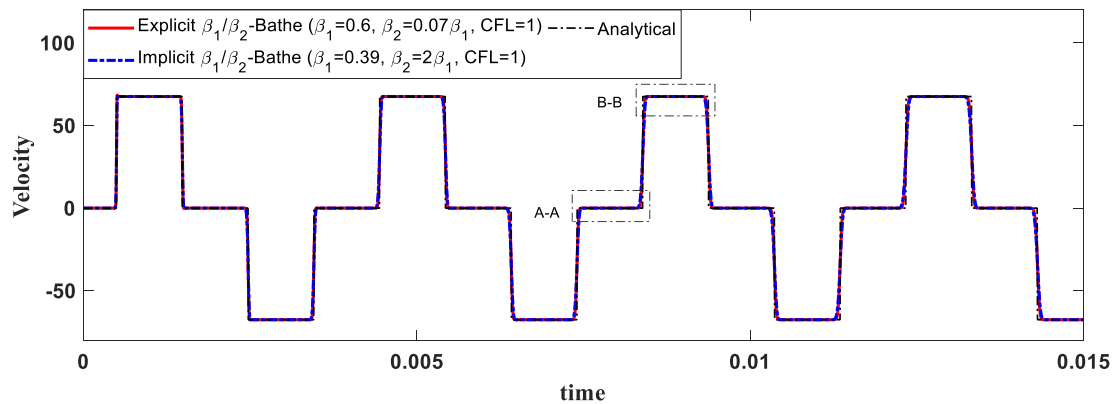


Fig. 14. Comparison of results when the explicit and implicit β_1/β_2 -Bathe methods are used, CFL = 1.0.

β_1/β_2 -Bathe method with the same CFL as with the Noh-Bathe method, that is CFL = 1.8519, gives slightly better results, but then using the smaller CFL = 1.5 very good results are obtained, which we do not obtain employing the Noh-Bathe method with CFL = 1.5. Similarly, the solution using the implicit β_1/β_2 -Bathe method with CFL = 1.8519 shows very good accuracy.

5.4. A pre-stressed square membrane

The pre-stressed square membrane shown in Fig. 29 is initially at rest when suddenly subjected to a constant unit initial velocity prescribed over its central domain (the gray area) with $L = 10$ m

and $l = 7$ m The wave velocity and mass density of the membrane are $c = 10$ m/s and $\rho = 1$ kg/m³, respectively. Due to symmetry, we only discretize a quarter of the membrane using 150×150 equal 4-node elements.

We use

$$\Delta t = \text{CFL} \times \frac{\Delta x}{c} = \frac{\text{CFL}}{300}$$

for the Noh-Bathe, explicit β_1/β_2 -Bathe and implicit β_1/β_2 -Bathe methods to obtain the velocity solution at the center point.

Figs. 30 to 34 show the performance of the different schemes. We use again the recommended value of $p = 0.54$ for the Noh-

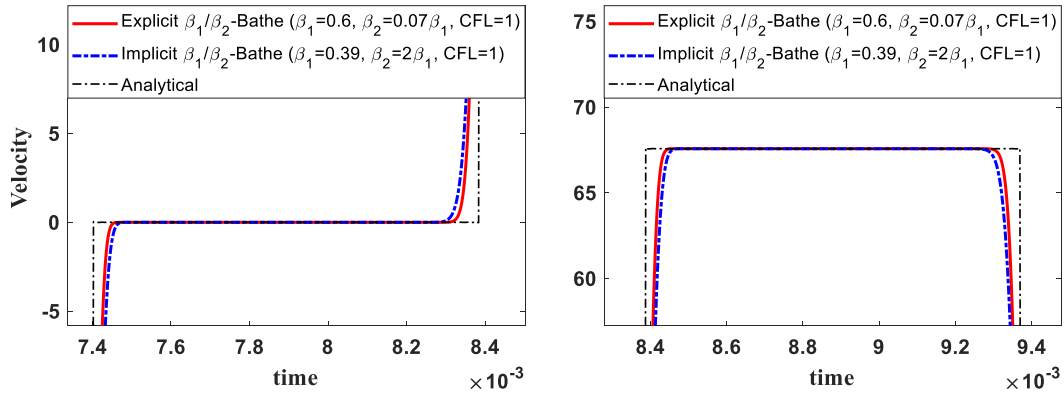


Fig. 15. Sections A-A and B-B of Fig. 14.

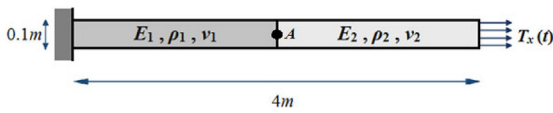


Fig. 16. A bi-material rod subjected to a step traction at its right edge.

Bathe method but also $p = 0.5858$ (also used in ref. [19]) resulting in $CFL = 1.7071$. As shown, the Noh-Bathe and explicit β_1/β_2 -Bathe methods yield good accuracy results with the β_1/β_2 -Bathe scheme giving slightly better results.

In Fig. 34 we show the solution obtained using the implicit β_1/β_2 -Bathe method and a smaller CFL, namely $CFL = 1.0$. Very good results have been obtained in this solution.

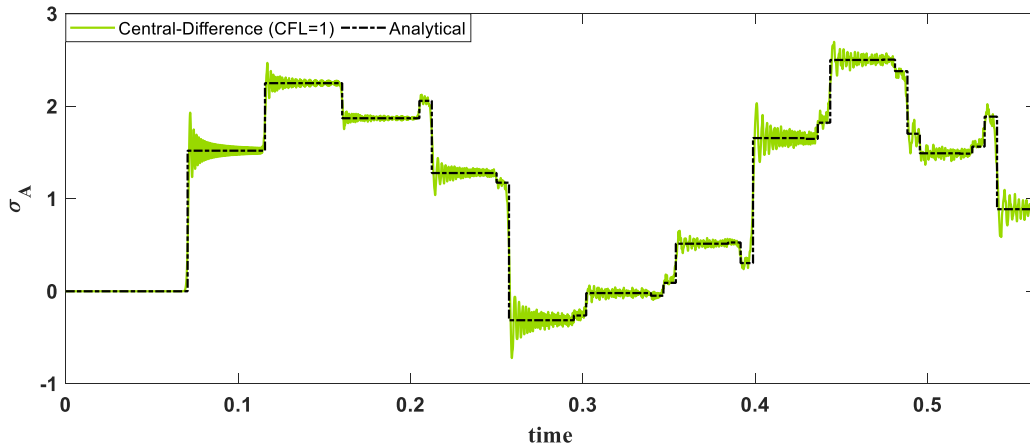


Fig. 17. Predicted stress at point A using the Central-Difference method.

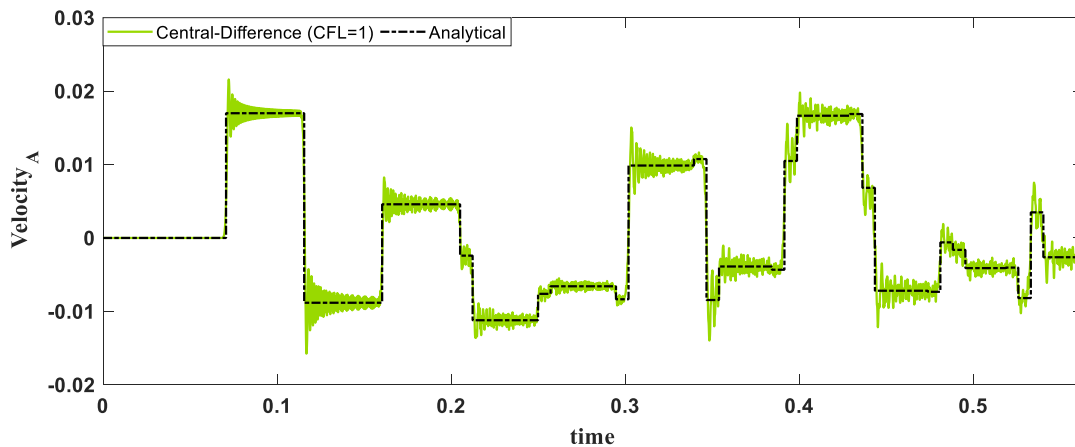


Fig. 18. Predicted velocity at point A using the Central-Difference method.

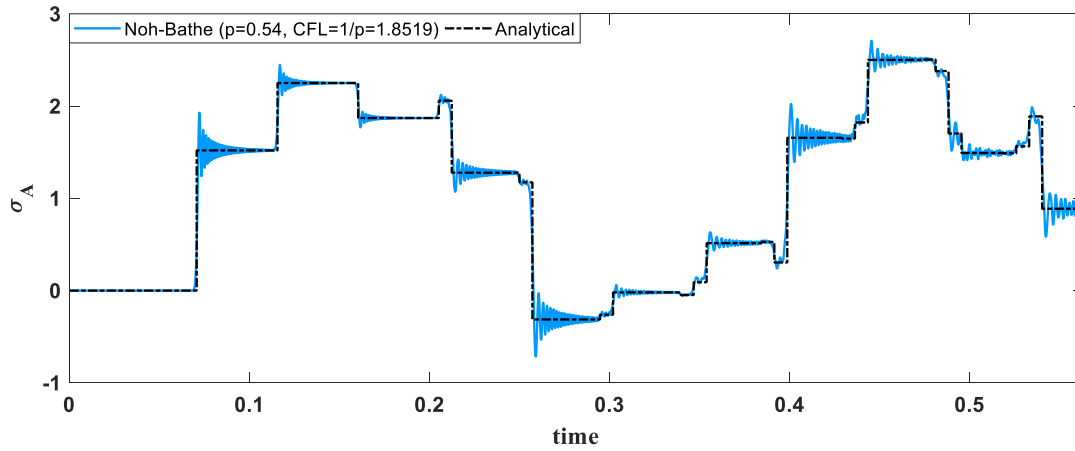


Fig. 19. Predicted stress at point A using the Noh-Bathe method, $p = 0.54$.

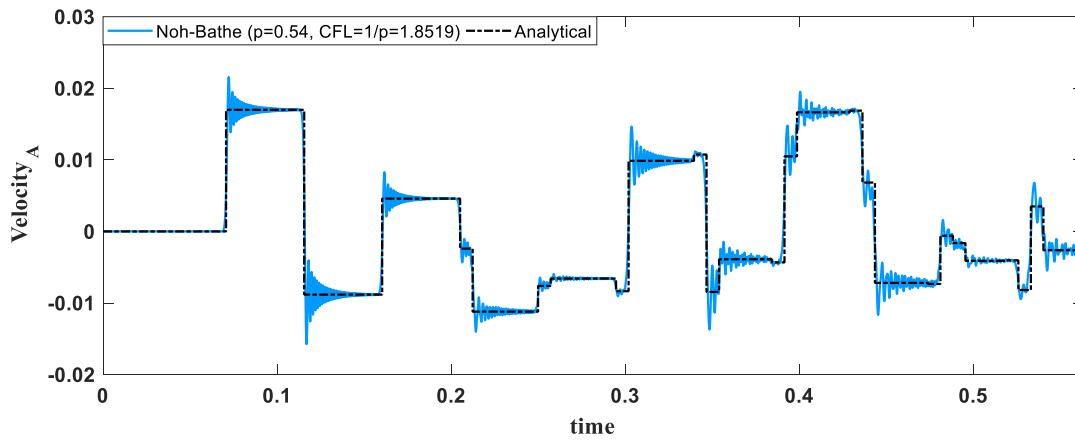


Fig. 20. Predicted velocity at point A using the Noh-Bathe method, $p = 0.54$.

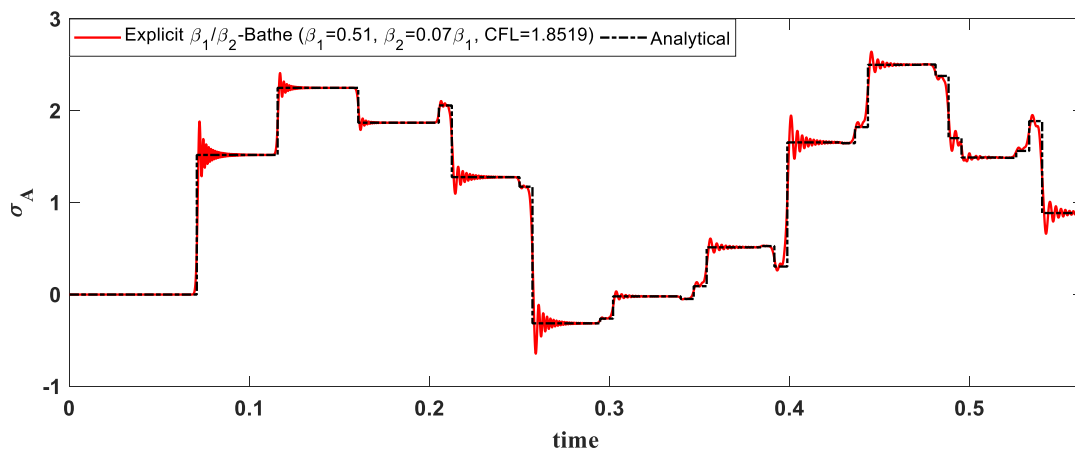


Fig. 21. Predicted stress at point A using the explicit β_1/β_2 -Bathe method, $CFL = 1.8519$.

6. Concluding remarks

The purpose of this paper was to introduce a new effective explicit direct time integration scheme, the explicit β_1/β_2 -Bathe method for solving dynamic problems, specifically wave propagations. Like the implicit Bathe schemes, the method uses two sub-

steps per time step. To obtain insight into the method, we mathematically analyzed the scheme with a focus on identifying the role of the two parameters β_1 and β_2 and their values. The analysis shows that the method can be used directly as a first-order or second-order scheme, with an effective ability to suppress the response due to high spurious frequencies.

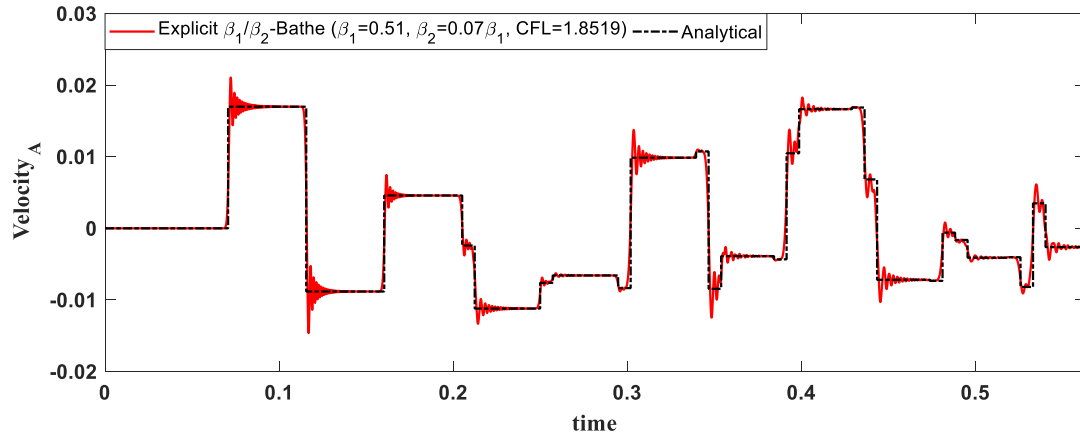


Fig. 22. Predicted velocity at point A using the explicit β_1/β_2 -Bathe method, CFL = 1.8519.

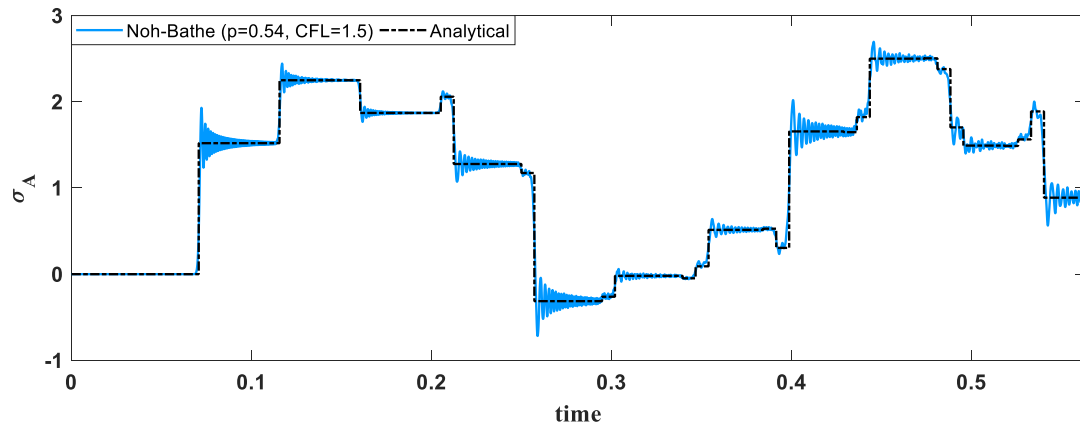


Fig. 23. Predicted stress at point A using the Noh-Bathe method, CFL = 1.5.

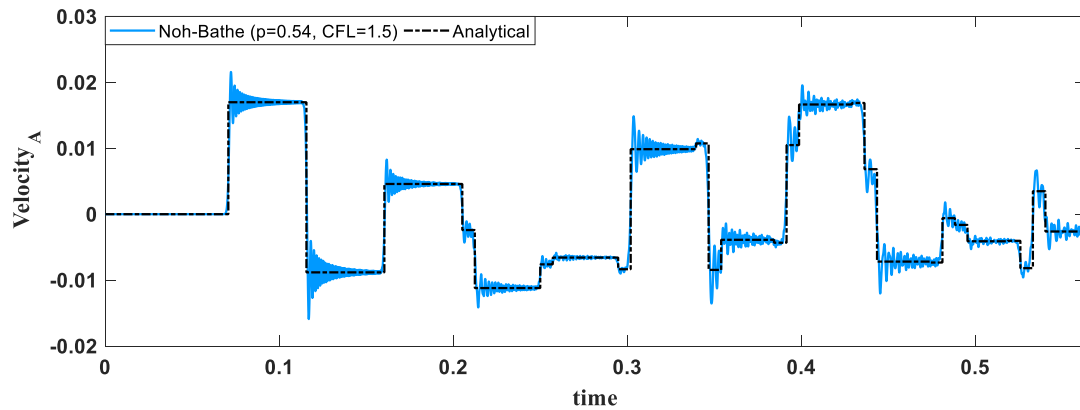


Fig. 24. Predicted velocity at point A using the Noh-Bathe method, CFL = 1.5.

To numerically demonstrate the properties of the explicit β_1/β_2 -Bathe method, we solved and compared in four problem solutions the results obtained using the proposed scheme with those calculated using the central difference and the explicit Noh-Bathe scheme. Based on the solutions obtained, we observed that the first-order explicit β_1/β_2 -Bathe method performs remarkably well even when focusing on the prediction of longer time response.

A comparison of the explicit β_1/β_2 -Bathe method with the Noh-Bathe scheme shows that the new method is in fact a further devel-

opment of and complements the Noh-Bathe scheme. In this paper we simply used the time splitting ratio γ to be 0.5, and further research is needed to establish the effect of changing this value (like in the Noh-Bathe scheme) to reach the full capabilities of this method designed for two unequal sub-steps, and to also establish the effect of physical damping.

However, to obtain the optimal, most accurate response prediction may require some numerical experimentation. Hence we give a table for choosing the values of β_1 and β_2 . Since a structural

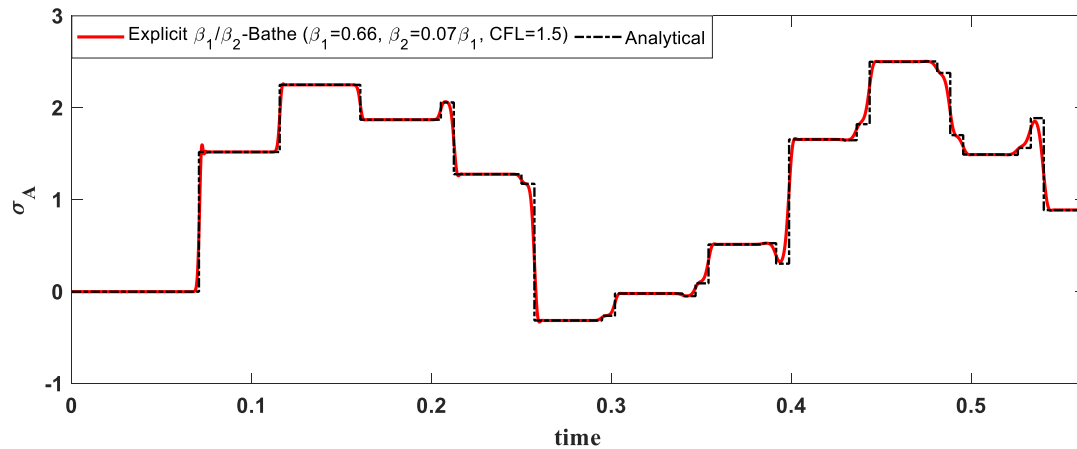


Fig. 25. Predicted stress at point A using the explicit β_1/β_2 -Bathe method, CFL = 1.5.

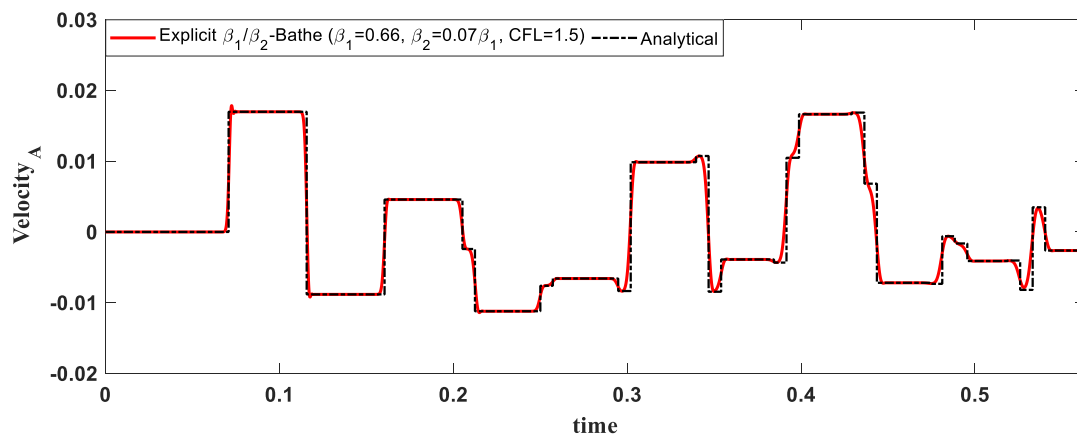


Fig. 26. Predicted velocity at point A using the explicit β_1/β_2 -Bathe method, CFL = 1.5.

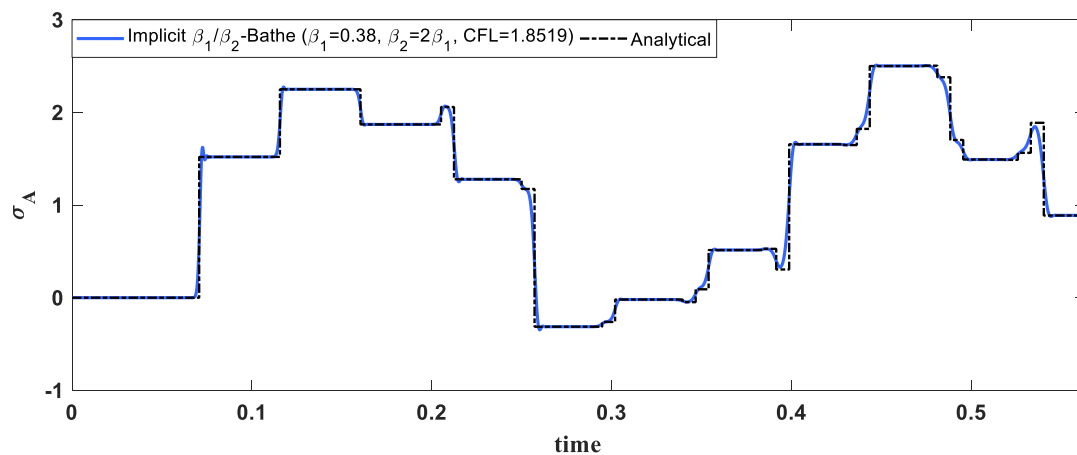


Fig. 27. Predicted stress at point A using the implicit β_1/β_2 -Bathe method, CFL = 1.8519.

response is fundamentally different from a wave propagation response, parameter values are given for each of these response calculations. In the first part of the table, ranges are given to choose from for optimal response predictions, and in the second part of the table, specific values are given to obtain in general quite accurate, but not necessarily most accurate, response predictions. Using the values in the second part of the table, we assume that no

numerical experimentation is performed (but can of course also be conducted). We used the values given in the table to demonstrate the solution accuracy of the scheme.

We have seen, in some problem solutions, that using the explicit β_1/β_2 -Bathe method, accurate response predictions were obtained due to the effective application of numerical damping. In practice, of course, spurious oscillations can frequently be seen

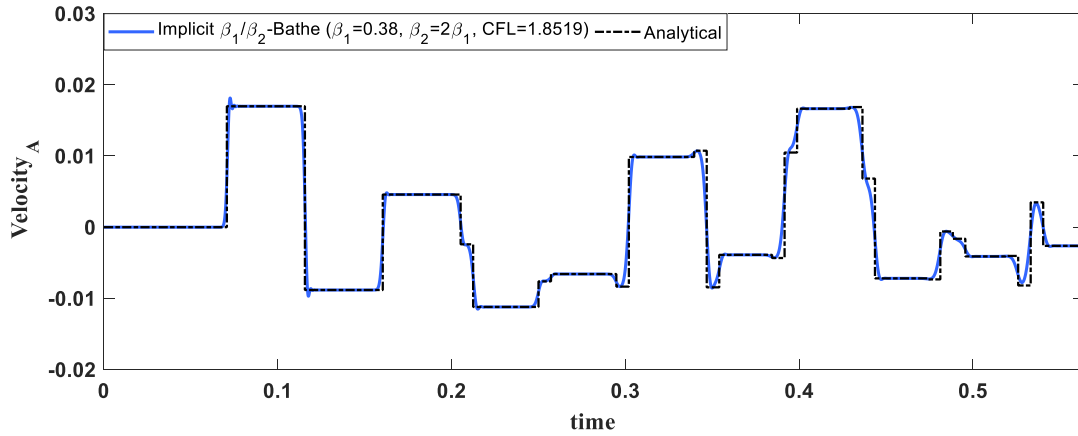


Fig. 28. Predicted velocity at point A using the implicit β_1/β_2 -Bathe method, CFL = 1.8519.

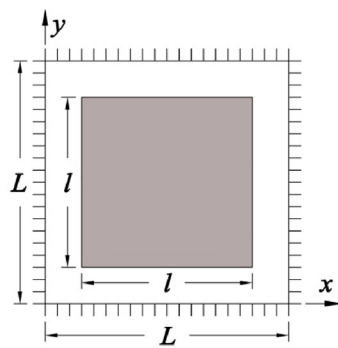


Fig. 29. The square membrane [16].

in numerical solutions, although no exact solution is available, and hence the proposed scheme gives means to suppress these oscillations.

Although we solved only linear problems, the scheme is fundamentally simple and can directly be applied to solve nonlinear problems as well.

However, for the “automatic optimal use” of the method further analyses, more insight, and more experiences with the use of the method are needed. The change of the splitting ratio γ and the analysis of the corresponding effects are of particular interest since additional benefits may be reached by taking full advantage of the two sub-steps used. This research may then lead to an automatic very effective solution algorithm.

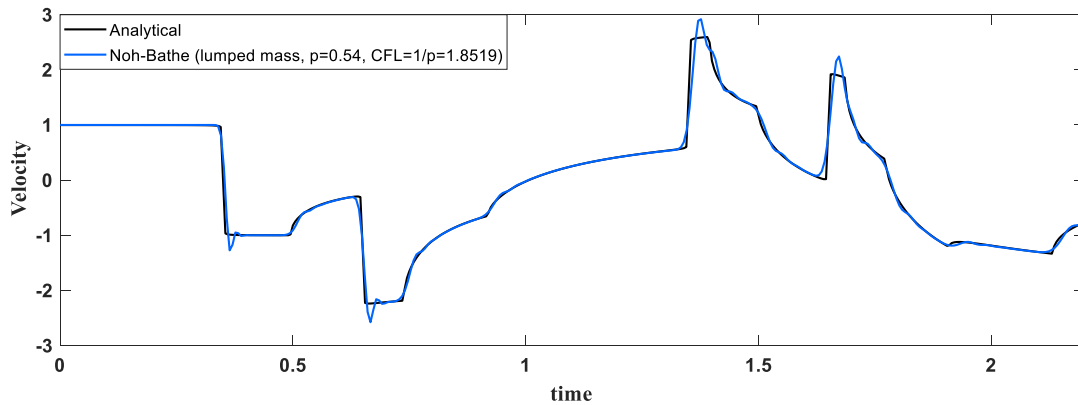


Fig. 30. Predicted velocity at center point using the Noh-Bathe method, $p = 0.54$.

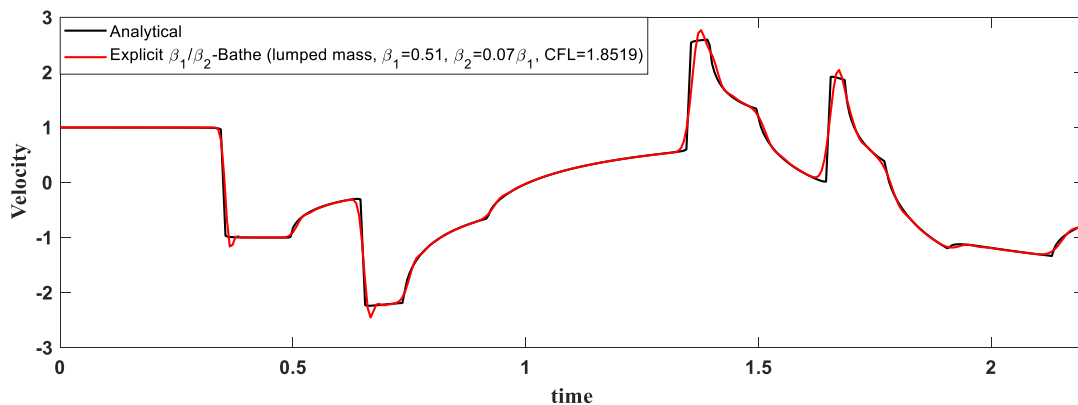


Fig. 31. Predicted velocity at center point using the explicit β_1/β_2 -Bathe method, CFL = 1.8519.

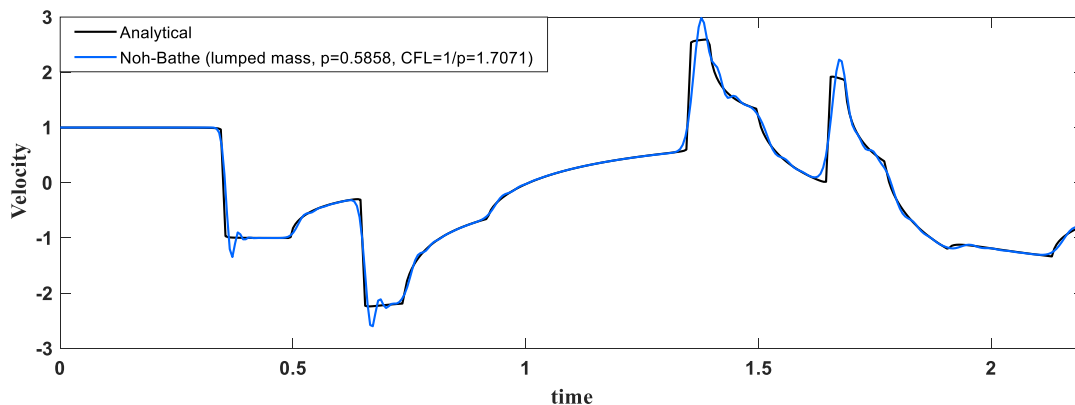


Fig. 32. Predicted velocity at center point using the Noh-Bathe method, $p = 0.5858$.

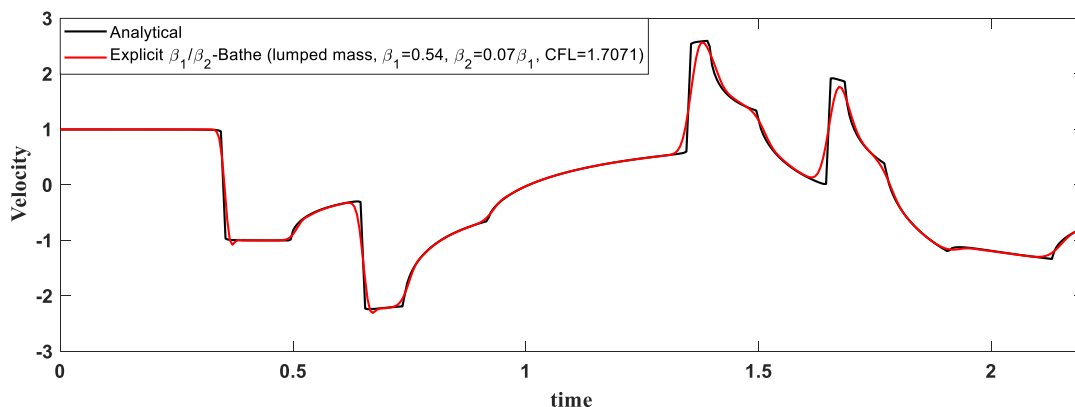


Fig. 33. Predicted velocity at center point using the explicit β_1/β_2 -Bathe method, $CFL = 1.7071$.

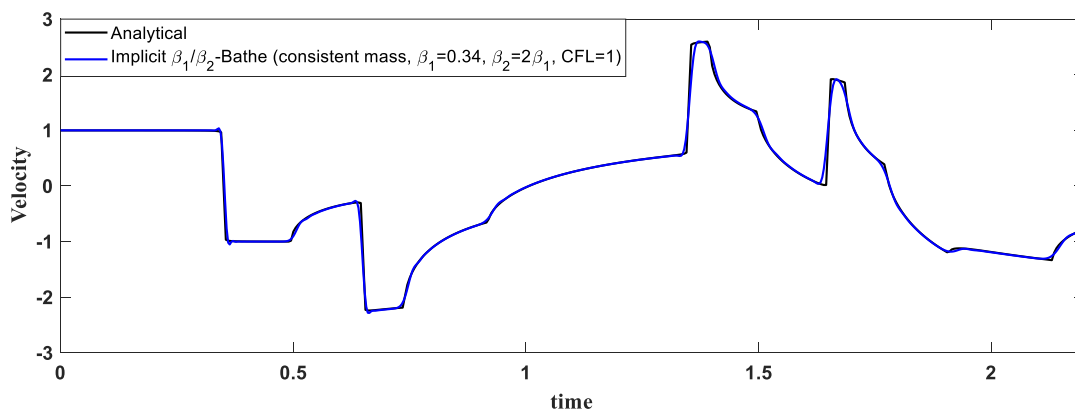


Fig. 34. Predicted velocity at center point using the implicit β_1/β_2 -Bathe method, consistent mass matrix, $CFL = 1$.

Data availability

No data was used for the research described in the article.

Declaration of Competing Interest

The authors declare that they have no known competing financial interests or personal relationships that could have appeared to influence the work reported in this paper.

Appendix A. Approximation operators of the proposed method

$$\begin{bmatrix} {}^{t+\Delta t}\ddot{u} \\ {}^{t+\Delta t}\dot{u} \\ {}^{t+\Delta t}u \end{bmatrix} = \mathbf{A} \begin{bmatrix} {}^t\ddot{u} \\ {}^t\dot{u} \\ {}^tu \end{bmatrix} + \mathbf{L}_a^{t+\gamma\Delta t}r + \mathbf{L}^{t+\Delta t}r \tag{23}$$

where

$$A = \begin{bmatrix} a_{11} & a_{12} & a_{13} \\ a_{21} & a_{22} & a_{23} \\ a_{31} & a_{32} & a_{33} \end{bmatrix}, L_a = \begin{bmatrix} Q_1 \\ Q_2 \\ Q_4 \end{bmatrix}, L = \begin{bmatrix} 1 \\ Q_3 \\ Q_5 \end{bmatrix} \quad (24)$$

$$\begin{aligned} b_1 &= -2\xi\omega(\gamma\Delta t) - 0.5\omega^2(\gamma\Delta t)^2 \\ b_2 &= -2\xi\omega - \omega^2(\gamma\Delta t) \\ b_3 &= -\omega^2 \\ b_4 &= (1 - \beta_1)(\gamma\Delta t) + \beta_1(\gamma\Delta t)b_1 \\ b_5 &= 1 + \beta_1(\gamma\Delta t)b_2 \\ b_6 &= \beta_1(\gamma\Delta t)b_3 \\ b_7 &= (\gamma\Delta t)^2((0.5 - \beta_2) + \beta_2b_1) \\ b_8 &= (\gamma\Delta t) + \beta_2(\gamma\Delta t)^2b_2 \\ b_9 &= 1 + \beta_2(\gamma\Delta t)^2b_3 \\ a_{11} &= -2\xi\omega b_4 - 2\xi\omega(\Delta t)(1 - \gamma)b_1 - \omega^2b_7 - \omega^2(\Delta t)(1 - \gamma)b_4 - 0.5\omega^2(\Delta t)^2(1 - \gamma)^2b_1 \\ a_{12} &= -2\xi\omega b_5 - 2\xi\omega(\Delta t)(1 - \gamma)b_2 - \omega^2b_8 - \omega^2(\Delta t)(1 - \gamma)b_5 - 0.5\omega^2(\Delta t)^2(1 - \gamma)^2b_2 \\ a_{13} &= -2\xi\omega b_6 - 2\xi\omega(\Delta t)(1 - \gamma)b_3 - \omega^2b_9 - \omega^2(\Delta t)(1 - \gamma)b_6 - 0.5\omega^2(\Delta t)^2(1 - \gamma)^2b_3 \\ a_{21} &= b_4 + (1 - \beta_1)(\Delta t)(1 - \gamma)b_1 + \beta_1(\Delta t)(1 - \gamma)a_{11} \\ a_{22} &= b_5 + (1 - \beta_1)(\Delta t)(1 - \gamma)b_2 + \beta_1(\Delta t)(1 - \gamma)a_{12} \\ a_{23} &= b_6 + (1 - \beta_1)(\Delta t)(1 - \gamma)b_3 + \beta_1(\Delta t)(1 - \gamma)a_{13} \\ a_{31} &= b_7 + (\Delta t)(1 - \gamma)b_4 + (0.5 - \beta_2)(\Delta t)^2(1 - \gamma)^2b_1 + \beta_2(\Delta t)^2(1 - \gamma)^2a_{11} \\ a_{32} &= b_8 + (\Delta t)(1 - \gamma)b_5 + (0.5 - \beta_2)(\Delta t)^2(1 - \gamma)^2b_2 + \beta_2(\Delta t)^2(1 - \gamma)^2a_{12} \\ a_{33} &= b_9 + (\Delta t)(1 - \gamma)b_6 + (0.5 - \beta_2)(\Delta t)^2(1 - \gamma)^2b_3 + \beta_2(\Delta t)^2(1 - \gamma)^2a_{13} \\ q_1 &= \beta_1(\gamma\Delta t) \\ q_2 &= \beta_2(\gamma\Delta t)^2 \\ Q_1 &= -2\xi\omega q_1 - 2\xi\omega(\Delta t)(1 - \gamma) - \omega^2q_2 - \omega^2(\Delta t)(1 - \gamma)q_1 - 0.5\omega^2(\Delta t)^2(1 - \gamma)^2 \\ Q_2 &= q_1 + (1 - \beta_1)(\Delta t)(1 - \gamma) + \beta_1(\Delta t)(1 - \gamma)Q_1 \\ Q_3 &= \beta_1(\Delta t)(1 - \gamma) \\ Q_4 &= q_2 + (\Delta t)(1 - \gamma)q_1 + (0.5 - \beta_2)(\Delta t)^2(1 - \gamma)^2 + \beta_2(\Delta t)^2(1 - \gamma)^2Q_1 \\ Q_5 &= \beta_2(\Delta t)^2(1 - \gamma)^2 \end{aligned} \quad (25)$$

References

[1] Bathe KJ. Finite element procedures: Prentice Hall; 1996, 2nd edition KJ Bathe, Watertown, MA, 2014; also published by Higher Education Press China 2016.
 [2] Dokainish MA, Subbaraj K. A survey of direct time integration methods in computational structural dynamics. I. Explicit methods. *Comput Struct* 1989;32(6):1371–86.
 [3] Subbaraj K, Dokainish MA. A survey of direct time integration methods in computational structural dynamics. II. Implicit methods. *Comput Struct* 1989;32(6):1387–401.
 [4] Newmark NM. A method of computation for structural dynamics. *J Eng Mec Div, ASCE* 1959;85(3):67–94.
 [5] Jia C, Bursi OS, Bonelli A, Wang Z. Novel partitioned time integration methods for DAE systems based on L-stable linearly implicit algorithms. *Int J Numer Meth Eng* 2011;87(12):1148–82.
 [6] Liua T, Huanga F, Wen W, He W, Duan S, Fang D. Further insights of a composite implicit time integration scheme and its performance on linear seismic response analysis. *Eng Struct* 2021;241:112490.

[7] Bathe KJ, Wilson EL. Stability and accuracy analysis of direct integration methods. *Int J Earthq Eng Struct Dyn* 1973;1(3):283–91.
 [8] Chung J, Hulbert GM. A time integration algorithm for structural dynamics with improved numerical dissipation: the Generalized-alpha method. *J Appl Mech Trans ASME* 1993;60:371–5.
 [9] Bathe KJ, Baig MML. On a composite implicit time integration procedure for nonlinear dynamics. *Comput Struct* 2005;83:2513–24.
 [10] Bathe KJ. Conserving Energy and Momentum in Nonlinear Dynamics: A Simple Implicit Time Integration Scheme. *Comput Struct* 2007;85:437–45.
 [11] Bathe KJ, Noh G. Insight into an implicit time integration scheme for structural dynamics. *Comput Struct* 2012;98:1–6.
 [12] Noh G, Bathe KJ. The Bathe Time Integration Method with Controllable Spectral Radius: the ρ_{∞} -Bathe Method. *Comput Struct* 2019;212:299–310.
 [13] Shojaee S, Rostami S, Abbasi A. An unconditionally stable implicit time integration algorithm: modified quartic B-spline method. *Comput Struct* 2015;153:98–111.
 [14] Malakiyeh MM, Shojaee S, Hamzehei-Javaran S. Development of a direct time integration method based on Bezier curve and 5th-order Bernstein basis function. *Comput Struct* 2018;194:15–31.
 [15] Malakiyeh MM, Shojaee S, Hamzehei-Javaran S. Insight into an implicit time integration method based on Bezier curve and third-order Bernstein basis function for structural dynamics. *Asian J Civil Eng* 2018;19(1):1–11.
 [16] Malakiyeh MM, Shojaee S, Hamzehei-Javaran S, Tadayon B. Further insights into time-integration method based on Bernstein polynomials and Bezier curve for structural dynamics. *Int J Struct Stab Dyn* 2019;1950113.
 [17] Malakiyeh MM, Shojaee S, Bathe KJ. The Bathe time integration method revisited for prescribing desired numerical dissipation. *Comput Struct* 2019;212:289–98.
 [18] Malakiyeh MM, Shojaee S, Hamzehei-Javaran S, Bathe KJ. New insights into the β_1/β_2 -Bathe time integration scheme when L-stable. *Comput Struct* 2021;245:106433.
 [19] Noh G, Bathe KJ. An explicit time integration scheme for the analysis of wave propagations. *Comput Struct* 2013;129:178–93.
 [20] Soares D. A novel family of explicit time marching techniques for structural dynamics and wave propagation models. *Comput Methods Appl Mech Eng* 2016;311:838–55.
 [21] Soares D. A novel time-marching formulation for wave propagation analysis: The adaptive hybrid explicit method. *Comput Methods Appl Mech Eng* 2020;366:113095.
 [22] Kim W, Reddy JN. Novel explicit time integration schemes for efficient transient analyses of structural problems. *Int J Mech Sci* 2020;172:105429.
 [23] Wood WL. Practical time-stepping schemes. Oxford: Clarendon Press; 1990.
 [24] Chung J, Lee JM. A new family of explicit time integration methods for linear and non-linear structural dynamics. *Int J Numer Methods Eng* 1994;37:3961–76.
 [25] Hulbert GM, Chung J. Explicit time integration algorithms for structural dynamics with optimal numerical dissipation. *Comput Methods Appl Mech Eng* 1996;137:175–88.
 [26] Chang SY, Liao WI. An unconditionally stable explicit method for structural dynamics. *J Earthquake Eng* 2005;9:349–70.
 [27] Noh G, Ham S, Bathe KJ. Performance of an implicit time integration scheme in the analysis of wave propagations. *Comput Struct* 2013;123:93–105.
 [28] Benitez JM, Montans FJ. The value of numerical amplification matrices in time integration methods. *Comput Struct* 2013;128:243–50.
 [29] Noh G, Bathe KJ. Imposing displacements in implicit direct time integration & a patch test. *Adv Eng Softw* 2023;175:103286.
 [30] Wood WL. Numerical integration of structural dynamics equations including natural damping and periodic forcing terms. *Int J Numer Meth Eng* 1981;17(2):281–9.